G. Droandi, G. Gibertini
Aerodynamic Blade Design with Multi-Objective Optimization for a Tiltrotor Aircraft
Aircraft Engineering and Aerospace Technology, Vol. 87, N. 1, 2015, p. 19-29
doi:10.1108/AEAT-01-2013-0005

Aerodynamic Blade Design With Multi-Objective Optimization For A Tiltrotor Aircraft

Abstract

Purpose – The aerodynamic design of tiltrotor blades is a very challenging task in the project of this type of aircraft. The purpose of this paper is to present the aerodynamic blade design of a tiltwing aircraft with a multi–objective optimization procedure.

Design/methodology/approach – Tiltrotor blades have to give good performance both in helicopter and aeroplane mode. According to the design parameters (the chords, the twists and the airfoils along the blade), since the optimization objectives are different from one operating condition to another, the blade is the result of a multi–objective constrained optimization based on a controlled elitist genetic algorithm founded on the NSGA–II algorithm. The optimization process uses a BEMT solver to compute rotor performance. To avoid negative effects due to compressibility losses in aeroplane mode, the blade shape has been refined following the normal Mach number criterion.

Findings – It has been found that the optimized rotor blade gives good performance both in terms of figure of merit and propulsive efficiency if compared with experimental data of existing rotor (ERICA tiltrotor) and propeller (NACA high–speed propeller).

Practical implications – The optimization procedure described in this paper for the design of tiltrotor blades can be efficiently employed for the aerodynamic design of helicopter rotors and aircraft propellers of all typology.

Originality/value – In this work, advanced methodologies have been used for the aerodynamics design of a proprotor optimized for an aircraft which belongs to the innovative typology of high–performance tiltwing tiltrotor aircraft.

Keywords Tiltrotor, Aerodynamic, Blade design, Multi–objective optimization.

Paper type *Research paper*.

Introduction

The tiltrotor concept, i.e. the idea of an aircraft that can behave both as an aeroplane and as a helicopter, is quite attractive due to its high versatility (Maisel et al., 2000; Gazdag and Altonin, 1990). The capability to convert from helicopter to aeroplane and vice versa is given by the tiltable rotors that are therefore called proprotors. Nowadays, an important focus point for future developments of this idea is the improvement of the performance in aeroplane mode, namely:

- increasing the maximum cruise speed;
- reducing the fuel consumption in cruise and increasing the operative range of the aircraft;
- allowing the possibility for take-off and landing as an aeroplane.

A possible approach to improve the aircraft performance in aeroplane mode is to reduce the rotor diameter and to increase the blade twist in order to get a propeller similar to the ones of turboprop aeroplanes. One direct consequence of this approach is the dramatic reduction of the aircraft hover performance. Thus, in order to preserve the performance in helicopter mode, non conventional tiltrotor configurations have to be further investigated (Alli et al., 2005; Gupta and Baeder, 2002).

These targets lead to the idea of a tiltwing as, for example, in the European project ERICA. The basic idea of ERICA (Alli et al., 2005; Gibertini et al., 2011) is the possibility to tilt a part of the wing (the part stroked by the rotor slipstream) to reduce the download effect on the wing and, consequently, to allow for smaller rotors that make the horizontal take–off and landing possible. This kind of solution has other advantages as it improves the performance in aeroplane mode (higher efficiency) and positively affects the width of the conversion corridor. This attracting and promising concept is still object of study and many aerodynamic aspects can be investigated in more depth . This paper presents the optimized design of a rotor developed for a tiltwing tiltrotor model that will be used to investigate the subject of aerodynamic interaction between rotors and wing for an aircraft of this typology.

The rotor blade aerodynamic design is a very critical task in the project of a tiltrotor aircraft. For an aircraft of this kind, the same propulsive system must be used both in helicopter and aircraft mode flight but the operative conditions are very different in the two modes. The thrust required to the rotors in helicopter flight mode in hovering essentially corresponds to the aircraft weight, while the thrust required in aeroplane flight mode is about a fifth of the hover thrust as it corresponds to the aerodynamic drag (McVeigh, 1986; Felker, 1992). On the other hand the inflow ratio λ is quite lower for the helicopter rotor with respect to the aeroplane propeller. The huge difference between operating flight conditions of helicopters and turboprops implies the need of appropriate strategies in tiltrotor blade design. An overview of the blade aerodynamic design of modern helicopter rotor have been provided by JanakiRam (2003) while an extensive review of design optimization procedures for helicopter design has been given by Celi (1999). In the field of propeller design, an

example of blade shape optimization for efficiency improvement has been given by Cho and Lee (1998). Pratical considerations and aerodynamic requirements for tiltrotor blade design have been discussed by McVeigh et al. (1983) who have also described the application and the results of a design methodology to define the replacement blades of the XV–15 tiltrotor. Paisley (1987) investigated the possibility to use an optimization process inside the aerodynamic design of rotor blades for high–speed tiltrotors, while Liu et al. (1990) suggested a procedure for the aerodynamic design of tiltrotor blades by means of numerical optimization. Aside from the chosen design strategy, the proprotor efficiency depends on many parameters. An extensive description of possible design parameters and their influence on proprotors' aerodynamic optimization have been given by Leishman and Rosen (2011).

In conclusion, the design of proprotors is more complex than in the case of helicopter rotor or aeroplane propeller because the design goals have to be selected to achieve a fair balance between helicopter and aeroplane mode flight performance. When more than one target has to be considered in an optimization process, two possible strategies can be followed: a single objective optimization with a weighted objective function that balances the different needs or a multi–objective optimization that deals with more than one objective. The advantage of the multi–objective optimization with respect to single–objective optimization is represented by the vectorial nature of the objective function, where the scalar components of the latter directly correspond to each selected objective (Deb, 2008). Moreover, since the multi–objective optimization procedure produces a final solution in terms of Pareto–optimal solutions (a set of optimal non–dominated solutions), the designer can compare the results and select the best compromised optimal solution for the analysed problem. A good example of the application of a multi–objective optimization procedure for the aerodynamic design of helicopter rotor has been described by Le Pape and Beaumier (2005).

In the present work a multi–objective optimization procedure has been adopted in the frame of the genetic optimization technique for the aerodynamic design of a tiltwing tiltrotor blades.

Objectives definition

Three different objectives have been selected for the multi–objective optimization procedure and, for each objective, an aircraft operating condition has been assumed. Following Liu et al. (1990), Paisley (1987) and McVeigh et al. (1983), the performance goals have been set in terms of overall efficiency of the rotor. In particular, the following design points have been chosen:

- Objective 1: Maximization of the hover Figure of Merit (FM);
- Objective 2: Maximization of the Propulsive Efficiency (η_{climb}) in vertical climb;
- Objective 3: Maximization of the Propulsive Efficiency (η_{cruise}) in cruise at high speed.

The first and the second objectives are related to the aircraft operating in helicopter configuration, while the third objective concerns the aeroplane flight mode. The previous points represent the scalar components of the objective function of the optimization process. In order to quantitatively define these operative conditions, a reference aircraft geometry and same general data of the whole aircraft have been assumed, defining an aircraft in the same class of ERICA (Alli et al., 2005). Aircraft weight and performance have been estimated by means of statistical approach as reported by Droandi et al. (2012). The optimization procedure has been carried out on three different objectives corresponding to three different flight conditions, shown in Table 1. To reduce the complexity of the optimization problem it was decided to fix the rotational speed Ω of each operating condition by comparison with existing tiltrotors (XV–15, Maisel et al. (2000), V–22, McVeigh (1986), ERICA, Alli et al. (2005)). The internal radiusR_i, that is 0.8 m, and the external radiusR_o, that is 3.7 m, while the number of blades for each rotor was fixed to 4. Due to the half-tilt wing configuration the aerodynamic rotor-wing interaction is so small (Droandi et al., 2012) that it has been neglected in the present optimization process. The absence of relevant interaction effects has then been confirmed by experiments (Droandi et al., 2013).

Flight Condition 1 (Helicopter)		
Rotor speed	Ω	58.6 rad/s
Altitude	h	0 m
Maximum take–off weight	W_{MTOW}	10900 kg
Required thrust for hover	$T_{r,1} = W_{MTOW}/2$	53464 N
Flight Condition 2 (Helicopter)		
Rotor speed	Ω	58.6 rad/s
Altitude	h	0 m
Maximum take–off weight	W_{MTOW}	10900 kg
Climb speed	V_∞	10 m/s
Wing-Fuselage Drag	D^{wf}	3215 N
Required thrust for climb	$T_{r,2} = W_{MTOW}/2 + D^{wf}/2$	55072 N
Flight Condition 3 (Aeroplane)		
Rotor speed	Ω	45.0 rad/s
Altitude	h	7500 m
Cruise speed	V_∞	170 m/s
Wing–Fuselage Drag	D^{wf}	22577 N
Required thrust for cruise	$T_{r,3} = D^{wf}/2$	11288 N

Table 1: Flight conditions considered during the optimization procedure.

Problem formulation

In the present work, the blade shape is the result of a multi–variable, multi–objective constrained optimization based on a controlled elitist genetic algorithm founded on NSGA–II (Deb, 2002; Deb, 2008), that finds minima of multicomponent objective function using genetic algorithm. At each iteration, the solver combines the previous population with an offspring population that is the result of binary crowded tournament selection, recombination and mutation operators. The resultant population, that is a combination of parent and offspring populations, is then sorted according to

a fast nondomination procedure and members of the new population are selected with a fast crowded distance estimation procedure that uses the crowded–comparison operator (Deb, 2002). An implementation of the NSGA–II is included in the Global Optimization Toolbox (MathWorks, 2012) of Matlab® and it has been used in the present work.

The mathematical formulation of the constrained multi–objective optimization problem can be written as follows:

Minimize:

$$\boldsymbol{F}(\boldsymbol{x}) = \left(f_m(\boldsymbol{x})\right)^T, \qquad m = 1, \dots, M, \tag{1}$$

subject to:

$$\begin{aligned} x_i^{LB} \le x_i \le x_i^{UB}, \quad & i = 1, \dots, N, \\ g_j(\boldsymbol{x}) \le 0.0, \quad & j = 1, \dots, J, \\ h_k(\boldsymbol{x}) = 0.0, \quad & k = 1, \dots, K, \end{aligned}$$

where $\boldsymbol{x} = (x_1, \dots, x_N)^T$ is the design variables array (or individual) and $\boldsymbol{F}(\boldsymbol{x})$ is the objective function that is composed by M scalar quantities, where M is the number of selected objectives. The design variables space D is clearly defined by imposing that each design variable x_i can take a value that is restricted between a lower x_i^{LB} and upper x_i^{UB} bound. Once the design variables array $\boldsymbol{x}$ meets the design bounds, the solution is a feasible solution inside the feasible solutions space S if the design criteria, expressed by the linear inequality $g_j(\boldsymbol{x})$and equality $h_k(\boldsymbol{x})$ constraint functions, are satisfied. In the present analysis, the blade design variables array $\boldsymbol{x}$ includes the blade span–wise distribution of chord length c_i, twist angle θ_i and airfoil shape index ASI_i. In particular, 9 sections have been identified along the blade span for a total number of 27 variables. The twist angle θ_i is defined as the angle between the hub plane and the section chord (positive nose up) with null collective pitch. Each section has been rotated around a reference axis passing through 0.25% of local chord (corresponding to the feathering axis). The goal of the optimization problem has been defined as the maximization of 3 objectives expressed in terms of 3 efficiency parameters (which vary between 0 and 1). Since the NSGA-II algorithm used in the present work finds minima of multicomponent objective function, the objective function $\boldsymbol{F}(\boldsymbol{x})$ has been written subtracting each scalar componentFM, η_{climb} and η_{cruise} from 1 (Deb, 1995). All design variables have been limited by a set of prescribed lower and upper bounds. Linear inequality constraints limit the maximum twist angle variations and chord rate of change between one section and the following one. To avoid abrupt changes in chord value near the root of the blade, the chord of the first blade section has been linked to the chord of the second section by a linear equality constraint. The same has been done for last two sections at the blade tip.

Objective function evaluation

Every time an individual $\boldsymbol{x}$ of a certain population P_i has to be evaluated during the optimization procedure, each scalar component of the objcetive function $\boldsymbol{F}(\boldsymbol{x})$ is computed by an aerodynamic solver, based on the BEMT, as

recommended by Leishman and Rosen (2011) because it is matematically parsimonious and agrees reasonably well with experimental data (Liu et al., 1990; Gur and Rosen, 2008). This very simple model (Leishman, 2006) is based on the blade decomposition in a span-wise series of sectional elements (BE) and on the corresponding rotor disk decomposition in a series of concentric annuli. For each blade element a 2D aerofoil aerodynamics approach is coupled, by means of a recursive approach, with the induced velocity obtained by the annular version of the disk actuator model (MT). Both the axial and the azimuthal (swirl effect, Glauert, 1935) components of the induced velocity are taken into account. At blade tip, were the annular theory underestimates the induced velocity, the Prandtl's tip loss function is emploied to account for the wake inflow effects (Goldstein, 1929). The blade global loads are computed as sum of the different blade elemet contributions. Since in the objective function rotor performance (FM, η_{climb} and η_{cruise}) have to be evaluated in different flight conditions, aerodynamic characteristics of airfoil sections have been previously stored in tables for a wide range of angles of attack, Reynolds and Mach numbers. The aerodynamic solver extracts interpolated values of lift coefficientC_l, drag coefficient C_d and pitching moment coefficientC_m, for every specified value of angle of attack, Reynolds and Mach number in the stored range. The database of the aerodynamic characteristics of airfoil sections used for the analyses have been generated collecting together wind tunnel data (when present in literature, expecially for NACA airfoils, Abbott and Doenhoff, 1949) and CFD results from two–dimensional simulations. For the m-th flight condition, the aerodynamic solver yields the estimated thrust T_m and power P_m given by the selected blade.

To compute the performance of rotor blades operating in one flight condition, it is first necessary to calculate the corresponding trim condition of the rotor (in terms of pitch blade angleθ_0, Leishman, 2006). Once the blade shape and the flight condition have been fixed, the trim condition is then computed by the aerodynamic solver. Since the calculation of the trim condition can be fundamental to the evaluation of the blade performance for a given flight condition$m$, the trim pitch angle is computed by the aerodynamic solver in order to satisfy the thrust required constraint$T_{m,r}$. The problem can be summarized as follows:

Find:

$$T_m \tag{2}$$

such that:

$$T_m(\theta_0) - T_{r,m} = 0.$$

The link between the pitch angle θ_0 and the thrust T given by a rotor is tipically non–linear, hence equation (2) is non–linear and it has to be solved in a suitable manner. As shown by Leishman (2006), the trim problem for an hovering rotor can be efficiently approached by an iterative calculation. Every time an individual is evaluated by the optimizer, the trim problem has to be solved 3 times, one for each flight condition. Figure 1 shows trim procedure flow chart.

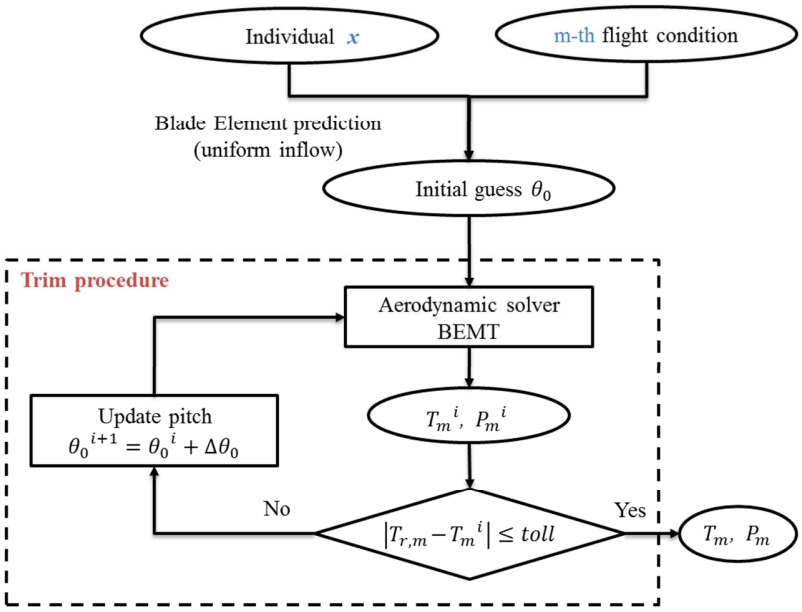

Figure 1: Rotor trim procedure for a selected flight condition.

Crossover and mutation functions

In order to manage a variables array that includes both real (the chord and the twist) and integer (the airfoil shape index) variables, same modifications of the tools of the Global Optimization Toolbox (MathWorks, 2012) have been done. Furthermore, appropriate crossover and mutation functions have been written in–house to improve the method efficiency. A scattered crossover operator has been used on pairs of parents, as shown by Michalewicz (1992), creating a random index vector to exchange the corresponding genes from one parent to the other and vice versa, to form pairs of childs. Sometimes, however, the crossover operator may give one or more offsprings outside of the feasible solutions space S (Michalewicz and Janikow, 1991). If this problem arises, thanks to convex solution spaces characteristics, a whole arithmetical crossover operator is used instead of scattered crossover operator. Individuals that are not recombined by the crossover operator (this number depends on the crossover fraction, choosen equal to 0.7 for the present analysis) are selected for mutation. In particular, following Neubauer (1997), an adaptive variant of the non–uniform mutation operator developed by Michalewicz and Janikow (1991) has been implemented.

Generation of initial population

In order to have good results in relatively short computational time, it has been decided to use a population size of 70 individuals per generation. To start the optimization procedure, an initial population P_0 is required. Poles et al. (2009) have shown that, if genetic information present in the initial population is not enough, the genetic algorithm can converge prematurely to a local optimal solution. Such problem can be fixed making use of a well–distributed initial population. Deb (2008) suggests to include in the initial population some feasible individuals already known. For these reasons, before

starting the multi–objective optimization, single objective constrained optimizations, that finds minima of scalar objective function using genetic algorithm, have been carried out for each objective. Then, the initial population P_0 of the multi–objective optimization has been created selecting the same number of best individuals from each final population of single objective optimizations. Figure 2 shows the optimization procedure flow chart.

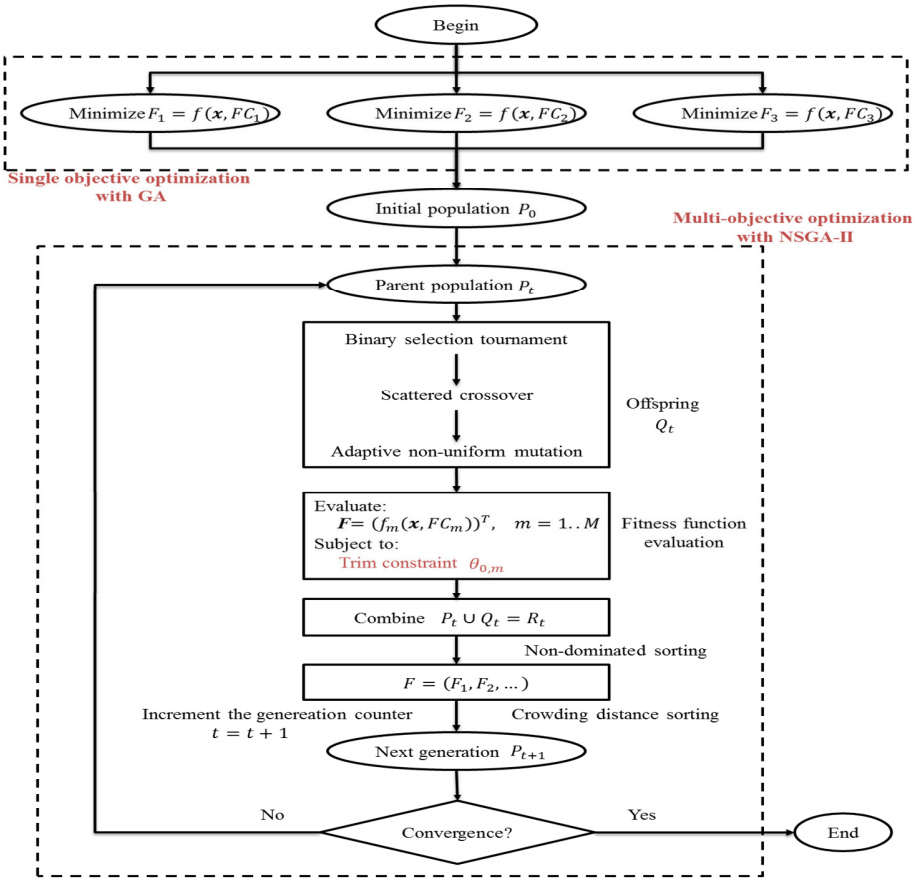

Figure 2: Rotor optimization procedure flow chart.

Blade optimization results

The multi–objective optimization procedure was ended after 400 iterations (28070 individuals have been evaluated) and the Pareto–optimal set resulted to be composed by 25 optimal individuals. In Figure 3 the Pareto–optimal front has been shown for each pair of objectives. Also the initial population P_0 has been reported in Figure 3 to show the improvements in terms of objective values due to the multi–objective optimization procedure. As it can be seen in Figure 3, the couple $f_1(\boldsymbol{x})$ and $f_2(\boldsymbol{x})$ represents slightly conflicting objectives while, on the other hand, they are both strongly conflicting with$f_3(\boldsymbol{x})$. The chosen blade, indicated with a red circle in Figure 3, is apparently the best compromise solution between all the solutions included in the Pareto–optimal set because it shows good performance in all flight conditions. In Table 2 a summmary of the predicted performance of the optimal blade I_0 has been reported for each flight condition

considered during the optimization process. In Figure 4 the selected optimal blade I_0 is compared with the individualsI_1, I_2 and I_3 included in the Pareto–optimal front and minimizing objective 1, 2 and 3 respectively. Figure 5 shows the resulting distribution of the optimization variables for these four blades. The data of the selected optimal blade I_0 are also listed in Table 3.

It is first apparent that the blade I_1 (the best one for the hovering) has a plant almost rectangular, similar to a typical helicopter blade, while the blade I_3 (the best one for the cruise) has a sensibly more “elliptic” and twisted shape, resembling a typical propeller blade. Looking at the load curves in hovering condition, as shown in Figure 6, it is clear that the blades I_0, I_1, I_2 have a good distribution (close to the ideal linear law for hovering rotor, Leishman, 2006) while the blade I_3 has a non-optimal behaviour. On the other hand, looking at the aeroplane cruise flight mode, as reported in Figure 7, it can be observed that the blade I_3 has a regular load distribution resembling the shape of optimal distribution for propellers (Goldstein, 1929). As for the other three solutions, only the blade I_0 has a reasonably similar behaviour while the blades I_1 and I_2 are clearly stalled toward the extremities. All the four presented solutions have the rotor inner part that does not give a positive contribution in aeroplane mode. In fact, the need to have also this part collaborating (and therefore not stalled) in the helicopter mode (where much more traction is required) leads to a blade twist quite lower respect to the need of a propeller, so producing negative incidences in aeroplane mode. On the other hand, at least for blades I_3 and I_0, the outer part of the rotor compensates adequately so that the global efficiency is nevertheless high.

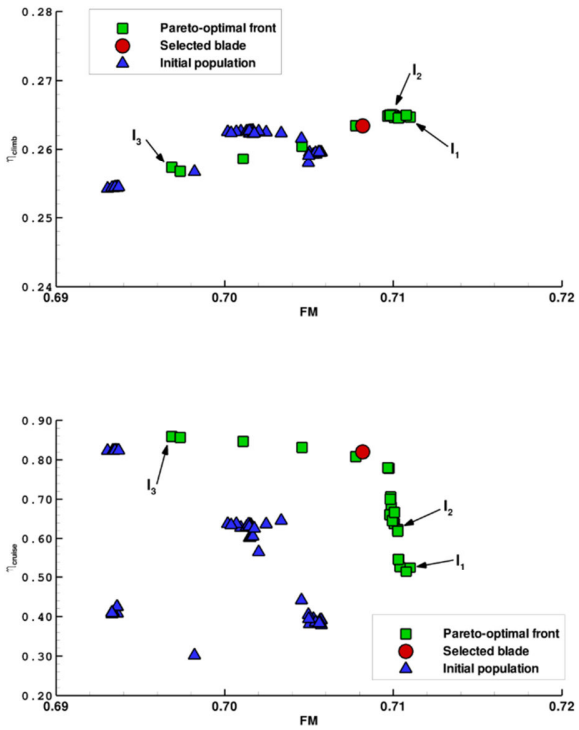

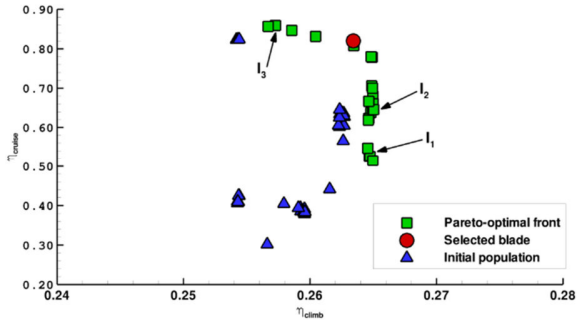

Figure 3: Pareto–front in the feasible solutions space. Comparison between Pareto–optimal front given by the multi–objective optimization procedure and initial population (created by single–objective genetic algorithm analyses).

	Flight Condition 1 (Helicopter)	Flight Condition 2 (Helicopter)	Flight Condition 3 (Aeroplane)
C_T	0.0215	0.0222	0.0169
C_P	0.00316	0.00388	0.0210
σ	0.194	0.194	0.194
θ_0 (°)	13.7	15.9	58.3
FM	0.709	-	-
η_{climb}	-	0.263	-
η_{cruise}	-	-	0.820

Table 2: Predicted performance of selected optimal blade I_0 from multi–objective optimization procedure.

Section number	r/R	c/R	θ (°)	Airfoil type
1	0.216	0.131	9.061	NACA 0030
2	0.270	0.133	8.351	NACA 0020
3	0.324	0.144	8.324	NACA 23014
4	0.487	0.168	5.217	VR–5
5	0.649	0.179	-0.005	OA–213
6	0.757	0.155	-2.265	VR–7
7	0.865	0.154	-2.849	VR–5
8	0.946	0.131	-3.540	RC–510
9	1.000	0.108	-4.759	RC–510

Table 3: Geometric parameters of the individual,I_0.

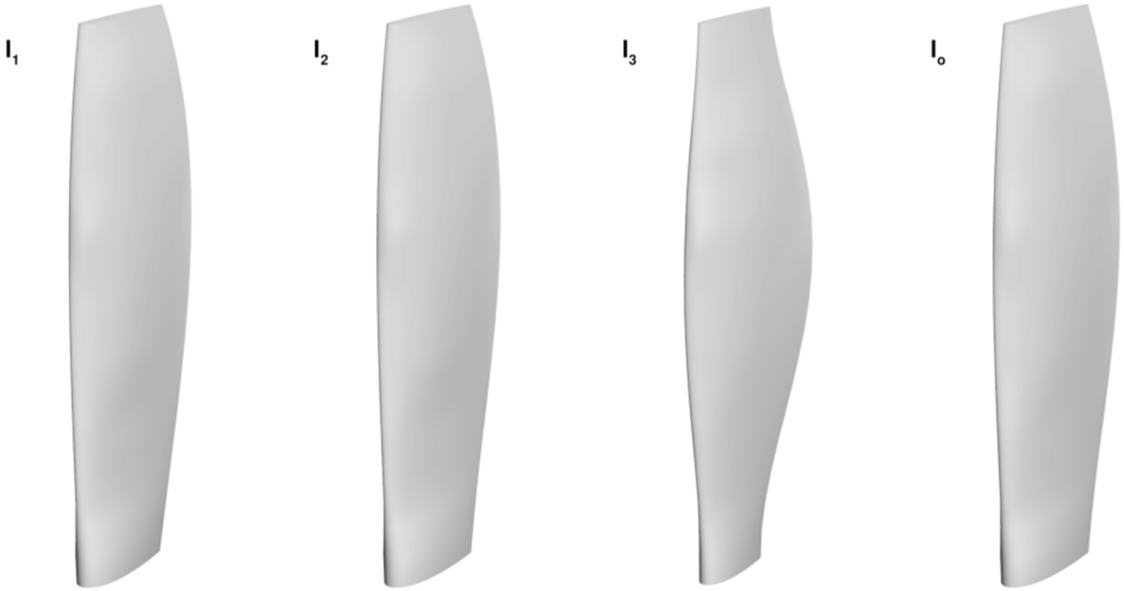

Figure 4: Blade geometry of individuals I_0, I_1, I_2, and I_3 from multi–objective genetic algorithm

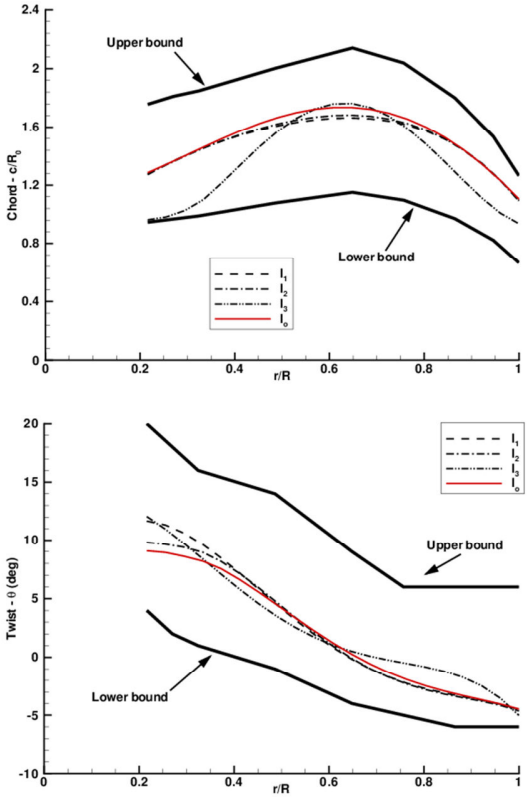

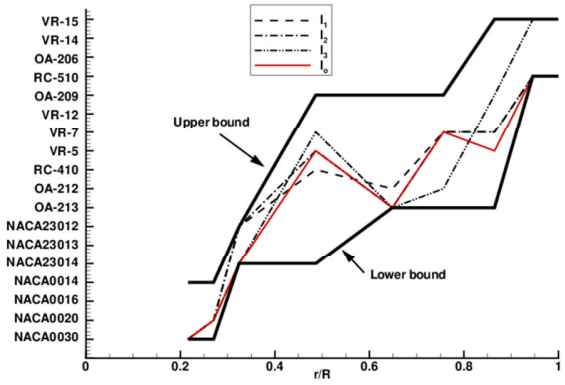

Figure 5: Optimized span–wise distribution of chord c_i, twist angle θ_i and airfoil shape index ASI_i using multi–objective genetic algorithm. Comparison between individual I_1, I_2, and I_3 and selected individual I_0 (from Pareto–optimal front).

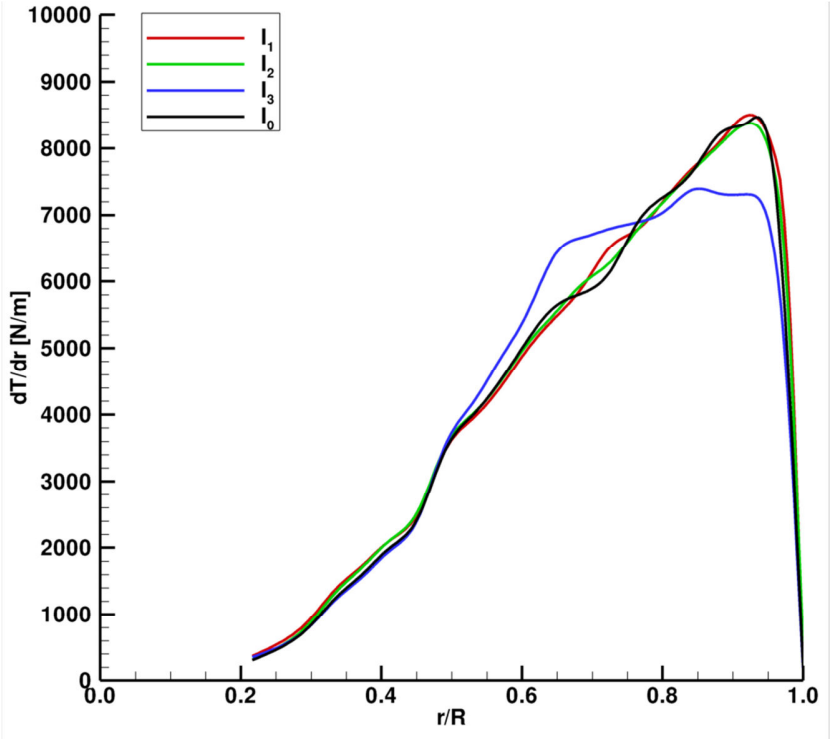

Figure 6: Span–wise distribution of thrust in hover flight condition. Comparison between individual I_1, I_2, and I_3 and selected individual I_0 (from Pareto–optimal front).

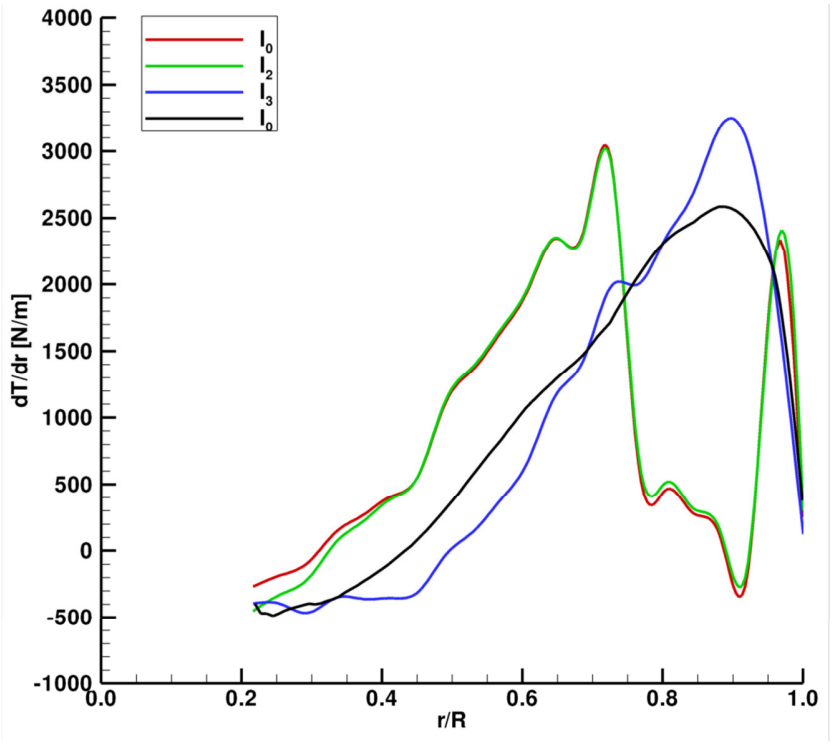

Figure 7: Span–wise distribution of thrust in cruise flight condition. Comparison between individual I_1, I_2, and I_3 and selected individual I_0 (from Pareto–optimal front).

Tip shape design

For a given rotational tip speed, by increasing the flight speed of a propeller, the helical Mach number increases and thus the compressibility effects arise on the blade. Thus, a progressive degradation of propeller performance becomes evident the higher the flight speed. Losses in propeller performance at high flight speed may depend on the airfoil sections and on the shape of the outer part of the blade. The most effective way to reduce power losses due to onset of compressibility effects is to sweep the blade tip following the normal Mach number criterion. Due to the fact that BEMT approach adopted in the optimization process is not capable to account for the sweep angle effects, this correction has been applied a posteriori to the selected optimal blade I_0 produced by the multi-objective optimizer. Hence the possible efficiency improvement had to be estimated by means of an high accuracy method.

The sweep angle distribution of the outer part of the blade has been calculated applying the normal Mach number criterion, which is similar to the method used for the sweptback wings (Shapiro, 1992). This criterion has been applied taking into account the cruise flight condition. The blade has been swept without modifying the airfoil shape, the chord and the twist of local sections that have been previously defined by the multi–objective optimization procedure. The backwards displacement of the outer sections of the blade moves the aerodynamic center of that sections behind the feathering axis. To keep the aerodynamic torsional moment limited and independent from the blade pitch angle variation, inboard blade

sections were swept upwards. The nondimensional position $\Delta\varsigma/R$ (positive in upward direction, Figure 8) of each section and the corresponding local sweep angle Λ are reported in Table 4. The comparisons between the planforms and the 0.25% chord curves of both the original blade I_0 (unswept) and its optimized version (swept) are shown in Figure 8.

Both the swept and the unswept blades have been finally evaluated with a compressible Navier–Stokes solver. Numerical simulations have been performed with the CFD code ROSITA developed at Politecnico of Milano (Biava et al., 2003, Biava et al., 2005, Biava, 2007). The code numerically integrates the unsteady RANS equations coupled with the one–equation turbulence model of Spalart–Allmaras (Spalart and Allmaras, 1992). Equations are formulated in terms of absolute velocity in overset systems of moving multi–block structured grids.

Thanks to the circumferential periodicity of the rotor geometry and its wake in the three flight conditions considered in this analysis, the simulations were carried out only on a 90° cylindrical sector with periodic boundary conditions on the sides. Numerical calculations have been performed both for the swept and for the unswept configurations of the optimal blade I_0 to predict the rotor performance in helicopter and aeroplane modes. Figure 9 and 10 show the comparison between the CFD results achieved for the swept and the unswept blade in hover and cruise flight conditions. The rotor performance, expressed in terms of FM and η_{cruise}, have been shown as function of C_T/σ. In both operating conditions the swept blade exhibits a small but not completely negligible increase of the rotor performance with respect to the unswept blade. The improvements in rotor efficiency are due to the introduction of the sweep angle distribution which decreases the negative effects due to onset of compressibility losses in the outer part of the blade. In particular, at the design point in hover ($C_T = 0.0215$), the FM of the swept blade is 0.720, that is 1.55% higher than the value of FM given by the unswept blade. In cruise flight condition, an increase of 1.46% in the η_{cruise} has been achieved at the design point ($C_T = 0.0169$) where the η_{cruise} of the swept blade is 0.831. In Figure 9 and 10 also the results given by the BEMT solver for the unswept blade are reported. The results of CFD simulations for the unswept blade are quite closer to the results of BEMT calculations (except for the smallest C_T/σ values in hover and the highest ones in cruise flight).

To evaluate the quality of the present results, the obtained rotor has to be compared with similar ones. Unfortunately public data about other proprotors of this kind are quite rare. The most obvious term of comparison is the rotor designed for the ERICA tiltrotor in the frame of TILTAERO (Viscardi et al., 2005) and ADYN (Bianchi et al., 2004) projects. Figure 11 shows that the present rotor generally has a higher hover efficiency with respect to the first version of the ERICA rotor (TILTAERO blades, Beaumier et al., 2008), while it presents a lower FM with respect to the final version of the ERICA rotor (ADYN blades, Beaumier et al., 2008). The same comparison for the aeroplane mode flight is not possible because public data on this condition are not available for the ERICA proprotor. Thus the optimized rotor has

been compared with a reference NACA high–speed propeller (Evans and Liner, 1958). Figure 12 shows that the optimized rotor has an η_{cruise} that is found to be similar to the corresponding value of a real high–speed propeller.

Section number	r/R	$\Delta\varsigma/R$	Λ (°)
1	0.216	0.000	0.0
2	0.270	0.000	0.0
3	0.324	0.000	0.0
4	0.487	0.003	-4.2
5	0.649	0.017	-4.4
6	0.757	0.025	-4.7
7	0.865	-0.003	23.9
8	0.946	-0.046	26.0
9	1.000	-0.077	27.3

Table 4: Geometric characteristics of the selected optimal blade I_0 geometry.

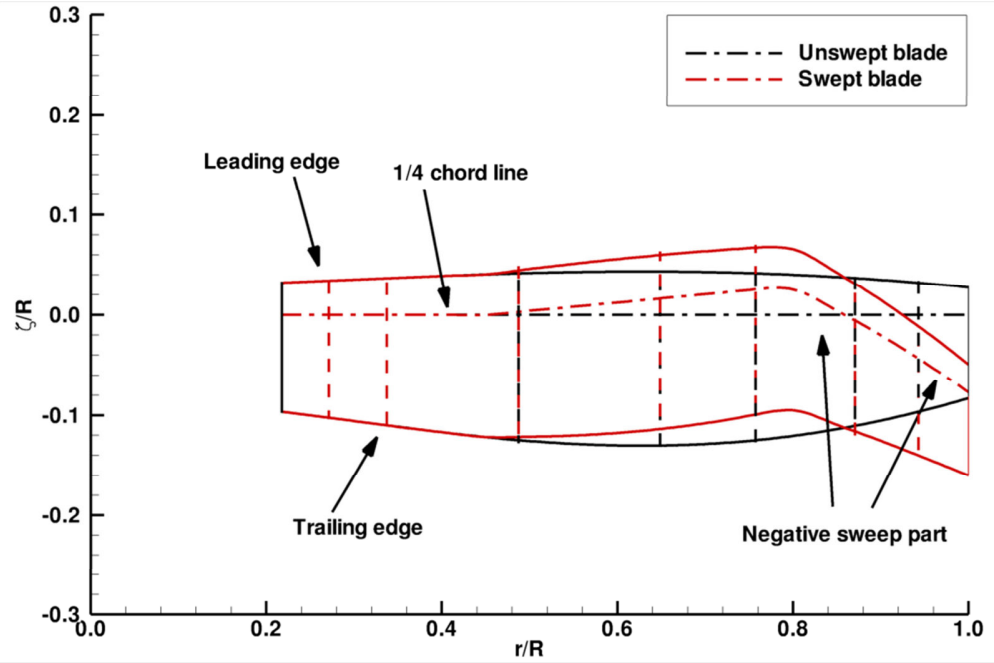

Figure 8: Optimized shape for compressibility losses of optimal rotor blade I_0.

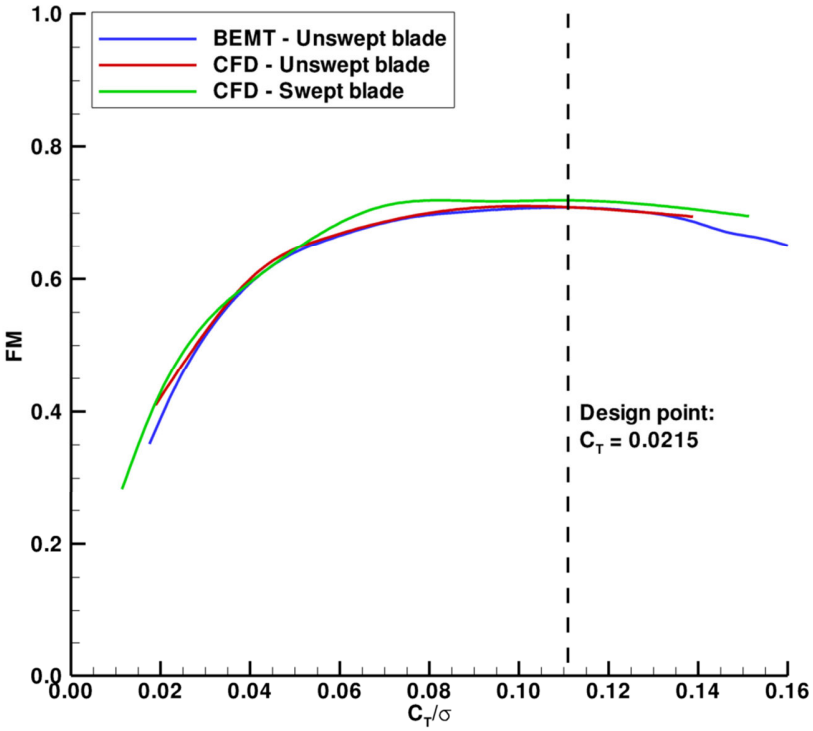

Figure 9: Comparison between swept and unswept configuration of selected optimal bladeI_0: hover performance, FM as function ofC_T/σ.

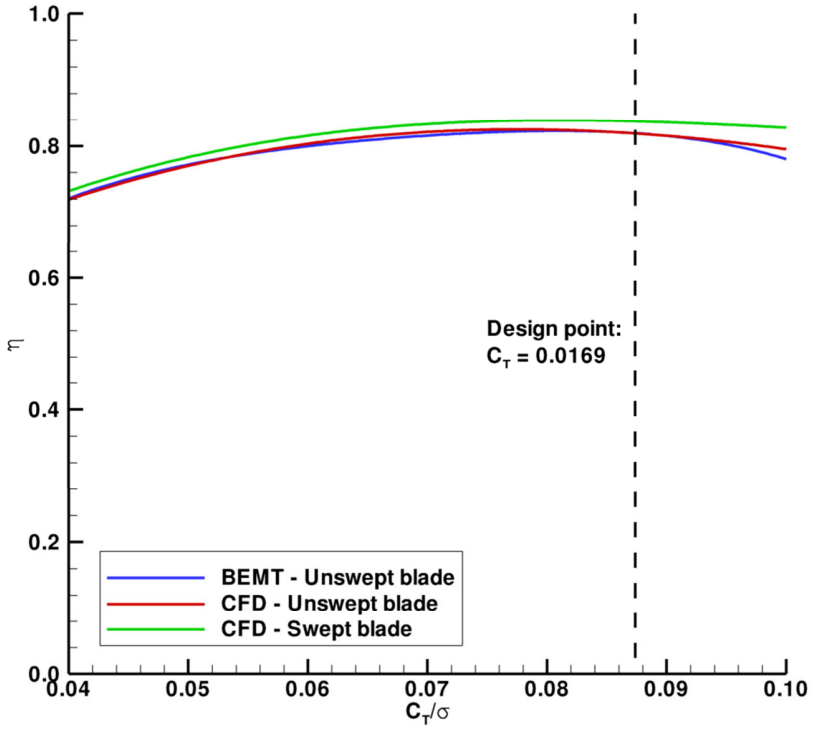

Figure 10: Comparison between swept and unswept configuration of selected optimal blade bladeI_0: hover performance, η_{cruise} as function ofC_T/σ.

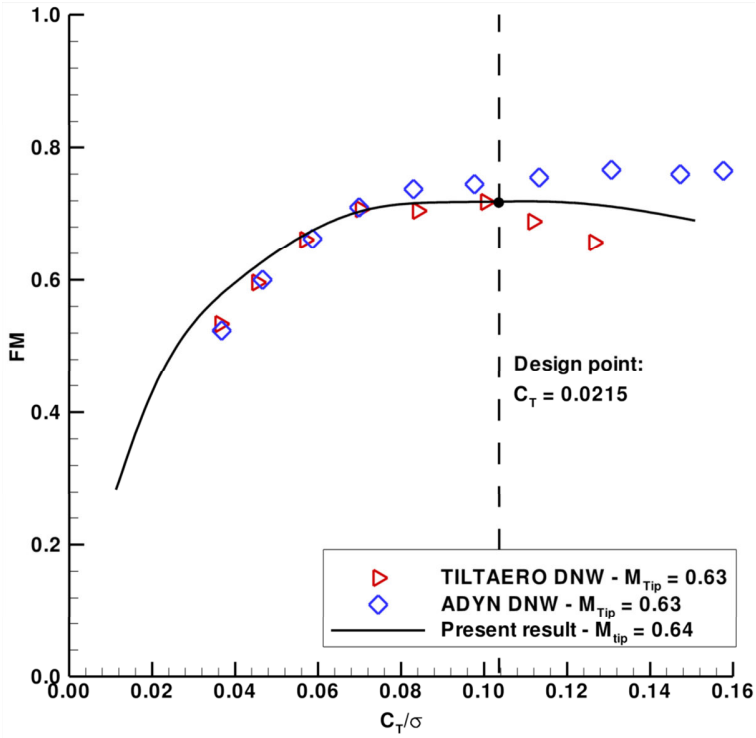

Figure 11: Rotor FM as function ofC_T/σ: comparison between predicted FM of selected optimal individual I_0 and hover tests data.

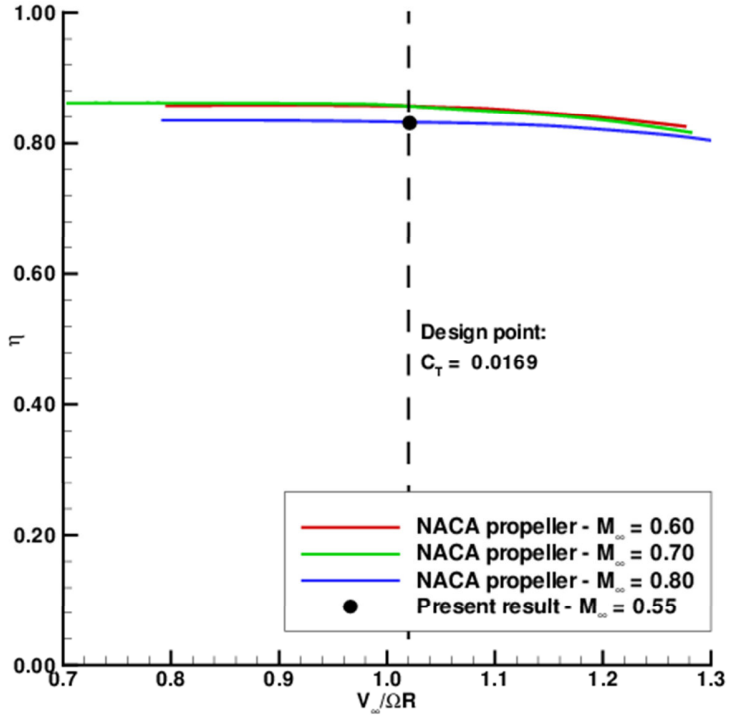

Figure 12: Rotor η as function of$V_\infty/\Omega R$: comparison between predicted η of selected optimal individual I_0 and wind–tunnel tests data.

Conclusions

An advanced optimization approach, based on a multi–objective optimization procedure, has been efficiently applied to the aerodynamic design of the rotor of an aircraft that belongs to the innovative typology of high–performance

tiltwing tiltrotor aircraft. The multi–objective optimization process is based on the NSGA–II algorithm and it has been coupled with a 2D aerodynamic solver (BEMT). To improve the optimizer efficiency, scattered crossover and non–uniform mutation funcions have been written ad hoc for the present problem and a well–distributed initial population has been generated by means of single objective optimizations. The optimal blade planform, which represent the best compromise in terms of performace between helicopter and aircarft flight modes, has been extracted from the final Pareto–optimal front. To reduce power losses due to onset of compressibility effects, the tip of the selected blade has been swept following the normal Mach number criterion. Both the swept and the unswept configurations of the optimal blade have been checked by means of a 3D compressible Navier–Stokes solver (ROSITA software).

The results for the unswept blade show a good agreement between CFD calculations and BEMT predictions both in hover and cruise flight conditions. The application of a non–linear sweep distribution to the straight blade shows the capability of the adopted metodology to improve the performance of the rotor. The final rotor geometry shows also good performance both in helicopter and aeroplane mode if compared with existing rotor and propeller.

The very different requirements for the very different flight conditions (i.e. helicopter and aeroplane mode) of a tiltrotor aircraft have been efficiently managed by the multi–objective optimization procedure. The comparisons between the final blade and existing rotor and propeller demostrate that the optimization method described in this paper can be used for the aerodynamic design of a rotor of high–performance tiltwing tiltrotor aircraft. However, in general this optimization procedure can be suitable for the aerodynamic design of helicopter rotors and aircraft propellers.

References

Abbott, I., Doenhoff, A. V. (1949), “Theory of Wing Sections, Including a Summary of Airfoil Data”, McGraw–Hill Book Co., Inc. (Reprinted by Dover Publications, 1959), New York.

Alli, P., Nannoni, F., Cicalè, M. (2005), “Erica: The european tiltrotor design and critical technology projects”, In: AIAA/ICAS. International Air and Space Symposium and Exposition: The Next 100 Years, 14–17 July, Day-ton, Ohio, USA.

Beaumier, P., Decours, J., Lefebvre, T. (2008) “Aerodynamic and aeroacoustic desing of moder tilt–rotors: the onera experience” In: ICAS. 26th International Congress of the Aeronautical Sciences, 14–19 September, Anchorage, Alaska, USA.

Bianchi, E., Russo, A., Kiessling, F., Ferrer, R., Dieterich, O., Frisoni, M. ., Bakker, R., Riziotis, V., Petot, D., Lanz, M. (2004), “Numerical whirl–flutter investigation of the european tiltrotor concept: current status and future prospects”. 30th European Rotorcraft Forum, 14–16 September, Marseilles, France.

Biava, M., Boniface, J.-C., Vigevano, L. (2005) “Influence of wind–tunnel walls in helicopter aerodynamics predictions”, 31st European Rotorcraft Forum, 13–15 September, Florence, Italy.

Biava, M., Pisoni, A., Saporiti, A., Vigevano, L. (2003) “Efficient rotor aerodynamics predictions with an euler method”, 29th European Rotorcraft Forum, 16–18 September, Friedrichshafen, Germany.

Biava, M. (2007), “Rans computations of rotor/fuselage unsteady interactional aerodynamics”. Ph.D. thesis, Politecnico di Milano.

Celi, R. (1999), “Recent Applications of Design Optimization to Rotorcraft – a survey”, Journal of Aircraft, Vol. 36, No. 1.

Cho, J., Lee, S. (1998), “Propeller Blade Shape Optimization for Efficiency Improvement”, Computer and Fluids, Vol. 27, No. 3, pp. 407–419.

Deb, K. (1995), “Optimization for Engineering Design: Algorithms and Examples”, Prentice–Hall of India Private Limited, New Delhi.

Deb, K. (2002) “A fast and elitist multiobjective genetic algorithm: NSGA-II”, IEEE Transactions on Evolutionary Computation Vol. 6, No. 2, pp. 182–197.
Deb, K. (2008), “Multi–objective optimization using evolutionary algorithms”, John Wiley and Sons Ltd, Southern Gate, Chichester, West Sussex, United Kingdom.
Droandi, G., Gibertini, G., Biava, M. (2012), “Wing–rotor aerodynamic interaction in tiltrotor aircraft”, 38th European Rotorcraft Forum, 4–7 September, Amsterdam, The Netherlands.
Droandi, G., Gibertini, G., Lanz, M., Campanardi, G., Grassi, D., Garbaccio, S. (2013) "Wing-Rotor Interactions on a 1/4 - Scale Tiltrotor Half-Model", 39th European Rotorcraft Forum, 3-6 September, Moscow, Russia.
Evans, A., Liner, G. (1958), “A wind–tunnel investigation of the aerodynamic characteristics of a full–scale supersonic–type three–blade propeller at mach numbers to 0.96”, Tech. Rep. TR–1375, NACA.
Felker, F. (1992), “Wing download results from a test of a 0.658-scale V–22 rotor and wing”. Journal of the American Helicopter Society, pp. 58–63.
Gazdag, D., Altonin, L. (1990), “Potential use of tiltrotor aricraft in canadian aviation”, Tech. Rep. TM–102245, NASA, Ames Research Center, Moffett Field, CA, USA.
Gibertini, G., Auteri, F., Campanardi, G., Macchi, C., Zanotti, A., Stabellini, A. (2011), “Wind tunnel tests of a tilt–rotor aircraft”, Aeronautical Journal, Vol. 115, 1167, pp. 315–322.
Glauert, H. (1935), “Airplane Propellers, Division L of Aerodynamic Theory”, Springer Verlag, Berlin, Germany.
Goldstein, L. (1929), “On the vortex theory of screw propellers”. Proceedings of the Royal Society of London. Series A, Containing Papers of a Mathematical and Physical Character, Vol. 123 (792), pp. 440–465.
Gupta, V., Baeder, J. D. (2002), “Investigation of quad tiltrotor aerodynamics in forward flight using CFD”. In: AIAA. 20th AIAA Applied Aerodynamics Conference, 24–26 June, St. Louis, MO, USA.
Gur, O., Rosen, A, (2008), “Comparison between Blade-Element Models”, The Aeronautical Journal, Vol. 112, (1138), December 2008, pp. 689-704.
JanakiRam, R., Smith, R., Charles, B., Hassan, A. (2003), “Aerodynamic Design of a New Affordable Main Rotor for the Apache Helicopter”. 59th Annual Forum of the American Helicopter Society, Phoenix, Arizona, USA, May 6-8.
Leishman, J. G., Rosen, K. M. (2011), “Challenges in the aerodynamic optimization of high-efficiency proprotors”, Journal of the American Helicopter Society, Vol. 56, No. 1, pp. 4–21.
Leishman, J. G. (2006), “Principles of Helicopter Aerodynamics”, Cambridge Aerospace Series, New York, NY 10013–2473, USA.
Le Pape, A., Beaumier, P. (2005), “Numerical Optimization of Helicopter Rotor Aerodynamic Performance in Hover”, Aerospace Science and Tecnology, Vol.9, No. 3, pp. 191–201.
Liu, J., Paisley, D. J., Hirsh, J. (1990), “Tiltrotor aerodynamic blade design by numerical optimization method”, 46th Annual Forum of the American Helicopter Society Aerodynamics, Washington, D.C., USA.
Maisel, M., Giulianetti, D., Dugan, D. (2000), “The history of the XV–15 tilt rotor research aircraft: from concept to flight”, Monographs in Aerospace History, 17 SP–2000–4517, NASA History Division, Washington, D.C., USA.
MathWorks, T. (2012) “Global optimization toolbox, User’s Giude”, http://mathworks.it, [Online; accessed 10–December–2012].
McVeigh, M. A., Rosenstein, H. J., McHugh, F. J. (1983), “Aerodynamic design of the XV–15 advanced composite tiltrotor blade”, 39th Annual Forum of the American Helicopter Society Aerodynamics, 9–11 May, St. Louis, MO, USA.
McVeigh, M. A. (1986), “The V–22 tiltrotor large–scale rotor performance/wing download test and comparison with theory”, Vertica, Vol. 10, No. 3/4, pp. 281–297.
Michalewicz, Z., Janikow, C. Z. (1991), “Handling constraints in genetic algorithms”. Proceedings of the Fourth International Conference on Genetic Algorithms, pp. 151–157.
Michalewicz, Z. (1992), “Genetic Algorithms + Data Structures = Evolution Programs”, Springer–Verlag Berlin Heidelberg.
Neubauer, A. (1997), “Adaptive non–uniform mutation for genetic algorithms”, Computational Intelligence Theory and Application 1226, pp. 24–34.
Paisley, D. J. (1987), “Rotor aerodynamic optimization for high speed tiltrotors”, 43th Annual Forum of the American Helicopter Society Aerodynamics, St. Louis, MO, USA.
Poles, S., Fu, Y., Rigoni, E. (2009), “The effect of initial population sampling on the convergence of multi–objective genetic algorithms”, Multiobjective Programming and Goal Programming: Theoretical Results and Practical Applications Vol. 618, No. 3, pp. 123–133.
Shapiro, A. (1992), “The Dynamics and Thermodynamics of Compressible Fluid Flow”, The Ronald Press Company, New York.
Spalart, P., Allmaras, S. (1992), “One equation model for aerodynamic flows”, In: AIAA 92-0439. 30th AIAA Aerospace Science Meeting & Exhibit, Reno, Nevada, USA.
Viscardi, A., Decours, J., Khier, W., Voutsinas, S. (2005), “Code–to–code comparisons for the blind–test activity of the tiltaero project”, 31th European Rotorcraft Forum, 13–15 September, Florence, Italy.

Nomenclature

Symbols

A = Rotor disk area, πR^2 (m^2)

ASI_i = *i*-th airfoil index variable (non-dimensional)

= Drag coefficient (non-dimensional)

c_i = *i*-th chord length variable (m)

C_l = Lift coefficient (non-dimensional)

C_m = Pitching moment coefficient (non-dimensional)

C_T = Thrust coefficient, $T/(\rho A\Omega^2 R^2)$ (non-dimensional)

C_P = Power coefficient,$P/(\rho A\Omega^3 R^2)$ (non-dimensional)

D = Design variables space

D^{wf} = Aircraft drag (wing–fuselage) (N)

$\boldsymbol{F}$ = Objective function

f_m = *m*-th objective function component

FM = Figure of merit, $C_T^{3/2}/\left(\sqrt{2}C_P\right)$ (non-dimensional)

g_J = Inequality constraint function

h_k = Equality constraint function

λ = Inflow ratio, $(V_\infty + v_i)/(\Omega R)$ (non-dimensional)

Λ = Sweep angle (°)

N_b = Number of blades (non-dimensional)

η = Propulsive efficiency, TV_∞/P (non-dimensional)

Ω = Angular speed (rad/s)

P = Power (W)

P_i = *i*–th population (non-dimensional)

R_i = Internal rotor radius (m)

R_o = External rotor radius (m)

ρ = air density (kg/m^3)

S = Feasible solutions space

σ = Rotor solidity, $cN_b/(\pi R)$ (non-dimensional)

T = Thrust (N)

T_r = Required thrust (N)

θ_I = *i*–th twist angle variable (°)

θ_0 = Trim pitch angle (°)

V_∞ = Flight speed (m/s)

v_i = Induced axial velocity (m/s)

M_{MTOW} = Maximum take–off weight (kg)

$\boldsymbol{x}$ = Solution array

$\Delta\zeta$ = Local displaced section (m)

$_{climb}$ = vertical climb flight

$_{cruise}$ = cruise flight at high speed

^{UB} = Variable lower bound

^{LB} = Variable upper bound

$_m$ = *m*-th flight condition

Definitions, Acronyms and Abbreviations

BE = Blade Element

BEMT = Blade Element Momentum Theory

CFD = Computational Fluid Dynamics

ERICA = Enhanced Rotorcraft Innovative Concept Achievement

MT = Momentum Theory

NSGA-II = Non-dominated Sorting Genetic Algorithm II

RANS = Reynolds Averaged Navier-Stokes

ROSITA = Rotorcraft Software ITAly